3D spin glass and 2D ferromagnetic ***XY*** model: a comparison

1997 J. Phys. A: Math. Gen. 30 7337

(http://iopscience.iop.org/0305-4470/30/21/010)

J. Phys. A: Math. Gen. **30** (1997) 7337–7347. Printed in the UK PII: S0305-4470(97)86006-4

3D spin glass and 2D ferromagnetic XY model: a comparison

David Iñiguez†‖, Enzo Marinari‡¶, Giorgio Parisi§+ and Juan J Ruiz-Lorenzo§*

† Departamento de Física Teórica, Universidad de Zaragoza, P San Francisco s/n. 50009 Zaragoza, Spain

‡ Dipartimento di Fisica and Infn, Università di Cagliari, Via Ospedale 72, 07100 Cagliari, Italy

§ Dipartimento di Fisica and Infn, Università di Roma, La Sapienza, P A Moro 2, 00185 Roma, Italy

Received 15 July 1997

Abstract. We compare the probability distributions and Binder cumulants of the overlap in the 3D Ising spin glass with those of the magnetization in the ferromagnetic 2D XY model. We analyse similarities and differences. Evidence for the existence of a phase transition in the spin glass model is obtained thanks to the crossing of the Binder cumulant. We show that the behaviour of the XY model is fully compatible with the Kosterlitz–Thouless scenario. Finite-size effects have to be dealt with carefully in order to differentiate between two very different physical pictures that can look very similar.

1. Introduction

The existence of a phase transition in the three-dimensional (3D) Ising spin glass has caused problems for more than two decades (see for example [1, 2] and references therein). Today there is clear numerical evidence favouring the existence of a low-temperature broken phase [3–5, 2], but a deeper understanding of the underlying physics is still absent. It is clear, for example, that one is very close to the lower critical dimension (LCD), but understanding the details of the influence of such an effect is problematic.

Determining, for example, the infinite-volume limit of the Edward–Anderson order parameter [6] (q_{EA}) has been beyond reach until very recently, and the existence of the phase transition (in both three and four dimensions) has been established by exhibiting the crossing of the finite-size Binder parameter. One was able to show (for the 3D case see [3, 4]) that curves of $g_L(T)$, $g_{L+1}(T)$ as a function of T would cross at $T_{\mathrm{c}}^{(L)}$, but it was impossible to determine the non-trivial limit of $g_L(T)$ for $L \to \infty$ at $T < T_{\mathrm{c}}$ (and in the same way it was impossible to determine the large-volume limit of q_{EA}). Only very recently have off-equilibrium techniques [7] and equilibrium simulations based on parallel tempering [8] allowed a statistically significant determination of the four-dimensional (4D) infinite-volume order parameter q_{EA}.

‖ E-mail address: david@sol.unizar.es
¶ E-mail address: marinari@ca.infn.it
+ E-mail address: giorgio.parisi@roma1.infn.it
* E-mail address: ruiz@chimera.roma1.infn.it

0305-4470/97/217337+11$19.50

We start here by noting that the behaviour of the Binder parameter $g_L(q)$ in the 3D spin glass is very reminiscent of the one in the two-dimensional (2D) XY model (without quenched disorder), $g_L(m)$ (here m is the magnetization). Even for quite large lattices the curves for different lattice volumes are well split in the high-T phase, but seem to merge rather than cross at low T. Only on very large lattices can one see a non-ambiguous (but always very small) crossing [3, 5]. The 2D XY model shows that the order parameter goes to zero very slowly when we take the thermodynamical limit.

The same type of effect could be appearing in the 3D Edward–Anderson spin glass, and in order to be sure one is dealing with a real phase transition with a non-zero order parameter one has to be very careful, and keep possible contamination under control. That is why we have decided to run a comprehensive comparison of the order-parameter distributions for the 3D Edward–Anderson spin glass and for the 2D XY model. A detailed paper by Binder [9], containing a study of the distribution functions for the Ising model, can be considered a methodological prototype for this type of analysis, and can be used as a nice introduction to the finite-size scaling techniques and ideas used in this setting.

Let us start by reminding the reader about some main points concerning the definition of the LCD. The lower and upper critical dimensions ($d_{\rm l}$ and $d_{\rm u}$ respectively) are important in qualifying a statistical system. $d_{\rm u}$ is the minimal dimension where mean-field predictions hold (apart from logarithmic corrections), while the LCD, $d_{\rm l}$, is the maximal dimension where the finite-T phase transition disappears. A typical example is the usual Ising model, with $d_{\rm l} = 1$ and $d_{\rm u} = 4$ [10].

Since a ϕ^3 term appears in the effective Hamiltonian of spin glasses (see [6, 11] and references therein) one expects the upper critical dimension to be $d_{\rm u} = 6$. One of the possible ways to determine the LCD is based on the determination of the critical exponent η. One starts from the two-point correlation function at the critical point, $T = T_{\rm c}$, that for $|\boldsymbol{x} - \boldsymbol{y}| \to \infty$ behaves as

$$\langle \phi(\boldsymbol{x})\phi(\boldsymbol{y})\rangle \simeq |\boldsymbol{x} - \boldsymbol{y}|^{-(d-2+\eta)}. \tag{1}$$

The LCD is defined by

$$d_{\rm l} - 2 + \eta(d_{\rm l}) = 0 \tag{2}$$

i.e. by the fact that there is no power-law decay of the two-point correlation function at the ($T = 0$) critical point. A (replica-symmetric) ϵ-expansion computation [12] gives

$$\eta = -\tfrac{1}{3}\epsilon + 1.2593\epsilon^2 + 2.5367\epsilon^3 \tag{3}$$

where $\epsilon \equiv (6 - d)$. At order ϵ one obtains the promising estimate $d_{\rm l} = 3$, that collapses when the higher-order contributions are included. This does not allow any real solution for $d_{\rm l} \leqslant 6$. It is clear that because there could be many causes for problems (for example, replica symmetric breaking and poor convergence of the ϵ-expansion) the ϵ-expansion is not helpful in determining the LCD.

Equation (2) allows an estimate of $d_{\rm l}$ based on numerical estimates of the η exponent. In four dimensions, with Gaussian couplings, one finds $\eta = -0.35 \pm 0.05$ [7], while in 3D $\eta = -0.40 \pm 0.05$ [5]. The variation of η with d is small, and it seems safe to estimate $d_{\rm l} \simeq 2.5$. Even if this result is somehow peculiar (since in the field theoretical approach [11] one does not see any trace of propagators with non-integer powers) it is confirmed by a mean-field-based analysis [13] where one builds up an interface and looks at its behaviour. This mean-field computation gives $d_{\rm l} = 2.5$, in excellent agreement with the numerical estimate.

Numerical simulations in 3D [3, 5, 2] have now clearly shown that there is a finite-T phase transition, i.e. that $d_{\rm l} < 3$. The broken phase is mean-field-like, and understanding it

in more detail will be the aim of this paper. It is also well established that in 2D one finds a $T = 0$ phase transition (see [2] and references therein). Summarizing, from state of the art numerical simulations one can deduce that $2 \leqslant d_l < 3$.

The fact that $d_u = 6$ is also well supported by numerical results [14, 15]. In $6d$ one cen determine mean-field exponents ($\gamma = 1$, $\beta = 1$ and $z = 4$) with good accuracy, with logarithmic corrections (that have been detected in the equilibrium simulations).

Here we will try to shed more light on the difficult numerical simulations of the 3D Edward–Anderson spin glass. The main problem is probably the fact that the system is very close to its LCD. So the apparent merging of the Binder parameters in the low-T region, that has only recently been disentangled to show a significant crossing [3–5], is dramatically reminiscent of the one observed in the case of a Kosterlitz–Thouless (KT) transition. We will try here to learn more about the effects of an anomalous situation such as the KT one, by looking, for example, at the Binder cumulant and to the overlap probability distribution $P(q)$. To do this we will discuss in some detail the structure of the order-parameter probability distribution in the 2D XY model without disorder. We will stress how similar to the 3D spin glass things are at a first level of analysis, and where the relevant differences can be found. It is also remarkable that the pure 2D XY model has a peculiar *ageing* behaviour [16]: ageing is one of the crucial features of spin glass systems, and its qualification is of large importance.

In the next section we will define our models, the physically observable quantities, and give details about our numerical simulations. In section 3 we discuss our results, by following, in parallel, the 2D XY model without disorder and the 3D spin glass. In section 4 we draw our conclusions.

2. Models, observables and simulations

We have studied the 2D XY model on a squared lattice. The volume is denoted by $V = L^2$, the Hamiltonian is

$$\mathcal{H} = -\sum_{\langle x,y\rangle} \cos(\phi_x - \phi_y) \tag{4}$$

where $\langle x, y\rangle$ denotes a sum over nearest-neighbour site pairs, ϕ is a continuous real variable, and periodic boundary conditions are imposed on the system. This model shows an *infinite-order* phase transition (with $\beta_c \approx 1.11$) [17], the KT transition. In accordance with the Mermin–Wagner theorem [10] there cannot be non-zero-order parameters: the magnetization in the thermodynamical limit is zero for all $T > 0$. The KT transition is characterized by a change in the behaviour of the two-point correlation function, which goes from the exponential decay of the high-temperature phase to the algebraic decay of the low-temperature phase. The whole low-temperature phase ($\beta > \beta_c$) is critical (the correlation length is infinite).

To simulate this model we have used the Wolff single-cluster algorithm [18]. The simulations have been run at five different values of β in the low-temperature phase: $\beta = 1.3, 1.4, 1.5, 1.7, 2.0$. For each value of β we have used the lattice sizes $L = 8, 16, 32, 64, 128, 256$. For each value of (β, L) we have used 200 000 iterations of the single-cluster algorithm, discarding the first half for thermalization. The total CPU time required has been approximately 1 month on a 100 MHz Pentium-based computer.

We have measured the probability distributions of

$$m_1 \equiv \frac{1}{V}\left|\mathrm{Re}\sum_x \exp(\mathrm{i}\phi_x)\right| \tag{5}$$

that we denote as $P_1(m_1)$. We call $m_1^{\max}$ the value of m_1 where $P_1(m_1)$ is at a maximum and takes the value $P_1^{\max} \equiv \mathrm{Max}[P_1(m_1)]$. We have looked in detail at the first and second moments of $P_1(m_1)$, $\langle m_1 \rangle$ and $\langle m_1^2 \rangle$. We have also computed the Binder cumulant of the $P_1(m_1)$ distribution:

$$B_1 = \frac{1}{2}\left(3 - \frac{\langle m_1^4 \rangle}{\langle m_1^2 \rangle^2}\right). \tag{6}$$

At low T one can study the XY model by using the spin-wave approximation that neglects the role of vortices (since they are suppressed at low T). In the $T \to 0$ limit all the spins point in the same direction, and (θ) is uniformly distributed, so that

$$\langle m_1^p \rangle = \frac{1}{2\pi}\int_0^{2\pi} \mathrm{d}\theta \, \cos^p \theta \tag{7}$$

and the Binder cumulant at $T = 0$ has the value

$$B_1(T = 0) = \tfrac{3}{4}. \tag{8}$$

To determine the relevant scaling behaviour we use the fact that, for the XY model, $\chi \simeq L^{2-\eta(T)}$ and $\langle m^2 \rangle \equiv \chi / L^2$, where in the spin-wave approximation

$$\eta(T) = \frac{T}{2\pi} \tag{9}$$

is the anomalous dimension of the field. Moreover, since $P_1(m_1)$ is a probability distribution, normalized to one, with non-zero maximum value $(m_1^{\max})$ (at least for finite values of the lattice sizes) and with $\langle m_1^2 \rangle \simeq L^{-\eta} \to 0$ (at finite temperatures) we have that†

$$P_1^{\max} m_1^{\max} \simeq 1 \tag{10}$$

independently of the lattice size, L. Since

$$m_1^{\max} \simeq \langle m_1 \rangle \simeq \langle m_1^2 \rangle^{1/2}$$

we conclude that

$$\begin{aligned} m_1^{\max} &\simeq L^{-\eta(T)/2} \\ \langle m_1 \rangle &\simeq L^{-\eta(T)/2} \\ \langle m_1^2 \rangle &\simeq L^{-\eta(T)} \\ P_1^{\max} &\simeq L^{\eta(T)/2}. \end{aligned} \tag{11}$$

The other model we have studied is the 3D Ising spin glass with quenched random couplings, J, distributed with a Gaussian law. The Hamiltonian is

$$\mathcal{H} \equiv -\sum_{\langle i,j \rangle} \sigma_i J_{i,j} \sigma_j \tag{12}$$

where the spin are defined on a 3D cubic lattice and $\langle i, j \rangle$ denotes a sum over nearest-neighbour pairs.

As usual [2] we have simulated two real replicas (σ and τ) with the same quenched couplings, and we have measured the overlap

$$q(\sigma, \tau) \equiv \frac{1}{V}\sum_i \sigma_i \tau_i \tag{13}$$

and its probability distribution

$$P(q) = \overline{\langle \delta(q - q(\sigma, \tau)) \rangle} \tag{14}$$

† In the rest of the paper the symbol $A \simeq B$ means $A = O(B)$.

where, as usual, we denote the thermal average with $\langle(\cdots)\rangle$, and the average over the disorder distribution with $\overline{(\cdots)}$. The Binder cumulant of the probability distribution $P(q)$ is

$$g \equiv \frac{1}{2}\left[3 - \frac{\overline{\langle q^4\rangle}}{\overline{\langle q^2\rangle}^2}\right]. \tag{15}$$

We have run $L = 4, 6, 8, 10, 12$ and 16 lattices with 2048, 2560, 512, 512, 2048 and 500 samples respectively. We have used the supercomputer APE-100 [19].

For simulating the spin glass model we have used the simple tempering method for small lattices ($L \leqslant 10$), and the parallel tempering scheme for large lattices ($L \geqslant 12$) (see [20, 21, 2] and references therein). Thanks to that we have kept the level of thermalization reached by the system under control, that is very good in all cases (for a discussion of the standard criteria of control see [21]). We have checked that the equalities established numerically in [4], and proven by Guerra [22] hold for our results, and that the $P(q)$ is well symmetric, supporting the reach of full thermalization.

3. Results

In figures 1 and 2 we show the Binder cumulant and the probability distribution of the 3D Ising spin glass. Let us discuss first the Binder cumulant. In figure 1 there are two different regions. In the high-temperature region the curves corresponding to different lattice sizes are clearly split (they tend to zero in the thermodynamical limit). At low temperature (i.e. for β larger than $\beta_c^{SG} \approx 1.0$), on small lattice sizes (up to $L = 10$) the curves coalesce, within our small error bars, into one. It is interesting to note that defining a Binder cumulant based on three different replicas [23] allows a somewhat easier determination of the critical behaviour.

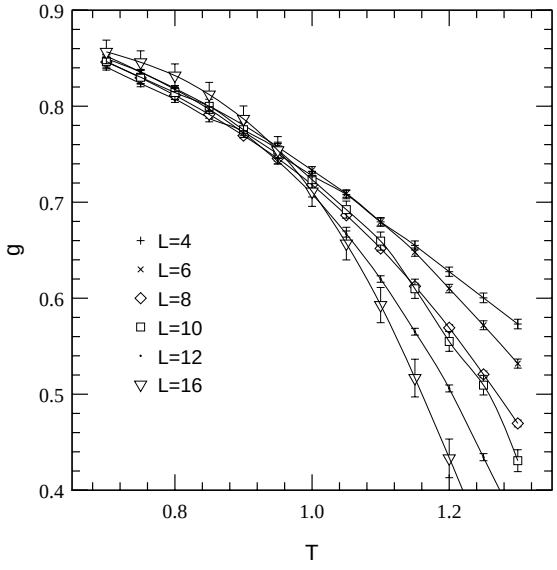

Figure 1. Binder cumulant for the 3D Ising spin glass. On the right, from top to bottom, curves and data points are for $L = 4$, 6, 8, 10, 12 and 16.

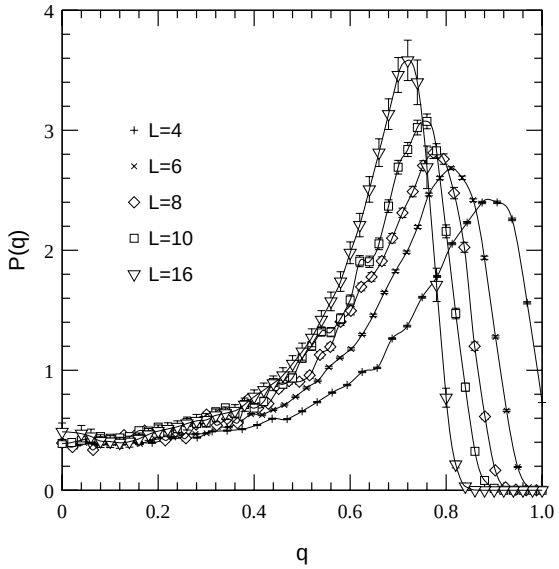

Figure 2. Probability distribution of the overlap, $P(q)$, for the 3D Ising spin glass ($T = 0.7$). From right to left the curves and data points are for $L = 4$, 6, 8, 10 and 16.

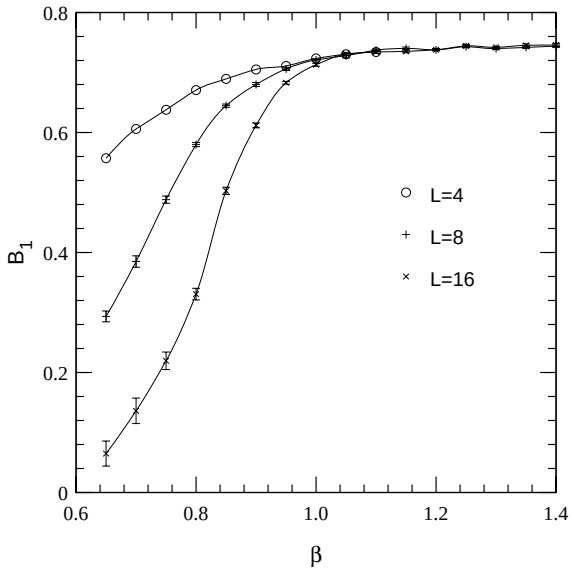

Figure 3. Binder cumulant, B_1, for the 2D XY model. From top to bottom, $L = 4$, 8 and 16.

Only when thermalizing an $L = 16$ lattice (quite large for current standards, and impossible to thermalize deep in the critical region without the use of parallel tempering [2]) one is able to distinguish a clear crossing between, for example, the $L = 8$ curve and the $L = 16$ curve. This implies the existence of a phase transition at finite temperature with a non-zero order parameter, $q_{\mathrm{EA}} \neq 0$ (see Kawashima and Young [3] for the model with quenched binary couplings, $J = \pm 1$).

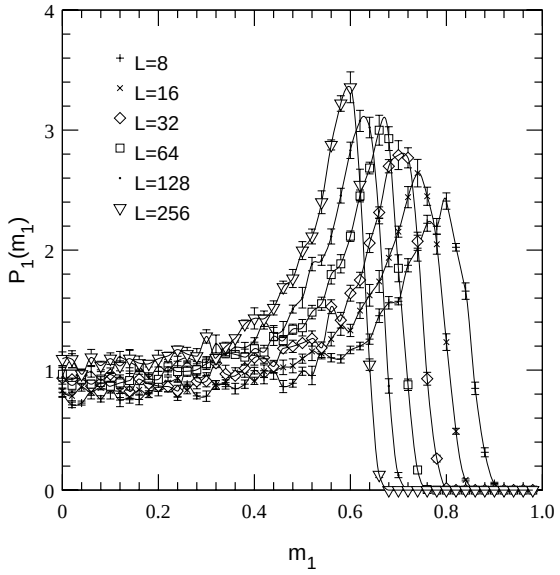

Figure 4. Probability distribution for the 2D XY model, $P_1(m_1)$, at $\beta = 1.3$.

Table 1. Numerical data for the 2D XY model, $\beta = 1.3$. See the text for further details.

L	$m_1^{\max}$	$\langle m_1 \rangle$	$\langle m_1^2 \rangle$	$P_1^{\max}$	$P_1(0)$
16	0.74(1)	0.485(6)	0.283(4)	2.64(9)	0.83(5)
32	0.70(1)	0.456(5)	0.260(3)	2.79(8)	0.93(2)
64	0.66(1)	0.431(5)	0.231(3)	3.00(9)	0.97(6)
128	0.62(1)	0.405(4)	0.205(2)	3.08(7)	0.94(9)
256	0.60(1)	0.382(5)	0.183(3)	3.36(11)	1.09(6)

We can compare figure 1 with figure 3, where we show our numerical results for the Binder cumulant, B_1, for the 2D XY model. Up to $L = 10$ the XY model and the 3D Ising spin glass have a very similar behaviour: again, within error bars, in the low-temperature region all the curves for different lattice sizes collapse in a single curve, without any visible sign of finite-size effects.

The behaviour of the full probability distribution of the order parameter (m_1 for the 2D XY model and q for the 3D Ising spin glass) is very similar. Figures 4 and 5, where we show $P_1(m_1)$ at $\beta = 1.3$ and $\beta = 2.0$ respectively, can be compared to the analogous figure 2 for the spin glass $P(q)$. The overall shapes are very similar. The peak shifts to the left and, in both cases, $P(0)$ looks constant in our statistical precision.

We give in table 1, at $\beta = 1.3$, the expectation values of the observables shown in figures 4 and 5. By fitting these values by using a single power fit we find

$$\begin{aligned} m_1^{\max} &\simeq L^{-(0.08\pm0.01)} \\ \langle m_1 \rangle &\simeq L^{-(0.09\pm0.01)} \\ \langle m_1^2 \rangle &\simeq L^{-(0.17\pm0.01)} \\ P_1^{\max} &\simeq L^{+(0.09\pm0.01)}. \end{aligned} \tag{16}$$

These results are in remarkable agreement within themselves and in good agreement with

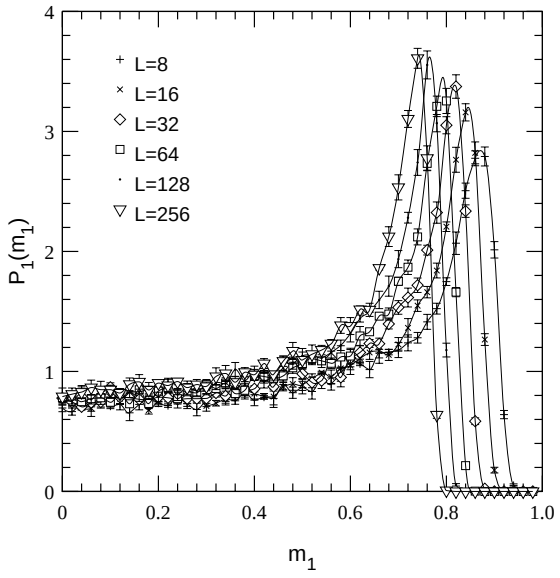

Figure 5. Probability distribution for the 2D XY model, $P_1(m_1)$, at $\beta = 2.0$.

the exact spin wave value $\eta(\beta = 1.3) = 0.12$. Corrections due to vortices are equivalent to a higher effective temperature [24], that here undergoes a 30% shift.

We have also established that a power fit to a non-zero infinite-volume order parameter of the form

$$m_1^{\max}(L) = m_1^{\max}(\infty) + \frac{A}{L^B} \tag{17}$$

with $m_1^{\max}(\infty)$ different from zero and A and B constant is excluded by the data.

Figures 4 and 5 are interesting: they show a finite-size non-trivial behaviour that we know, from theoretical ideas (the Mermin–Wagner theorem) and from the analysis of the numerical data, will converge to a zero centred delta-function distribution in the infinite-volume limit. This is the point we want to stress. Since the 3D spin glass has a very similar behaviour (and even for the 4D model, where the crossing of the Binder cumulant is clear, it is non-trivial to show that q_{EA} tends to a non-zero limit) it is crucial to understand where the differences appear.

We also want to stress that $P_1(m_1)$ shows a clear plateau, roughly L-independent, close to the $m_1 \simeq 0$ region. The plateau height grows with the lattice size (in a statistically significant way in our numerical data, see figure 1). This is one of the interesting results to note: the infinite-volume 2D XY m_1 delta function is constructed from the increasing finite volumes by a finite m_1 peak that shifts towards $m_1 \simeq 0$, and by a plateau in the $m_1 \simeq 0$ region that slowly increases with the lattice size, to eventually match the peak in the $m_1 = 0$ delta function.

We have repeated this analysis for the overlap probability distribution $P(q)$ of the 3D spin glass (see figure 2). The best scaling fit of the peak position, q_{M}, where the probability distribution is maximum, by a power law (the data are shown in table 2) gives

$$q_{\mathrm{M}} = (0.70 \pm 0.02) + (1.6 \pm 0.7)L^{-(1.5\pm0.4)} \tag{18}$$

where $T = 0.7$. In this fit we have used all lattice volumes ($L \leqslant 16$). The fit had a $\chi^2/\mathrm{dof} = 0.15$. This thermodynamical value we get for q_{EA} is close to the value that has

Table 2. Numerical data for the 3D Ising spin glass, $T = 0.7$. See the text for further details.

L	q_{M}	$P(0)$
4	0.91(1)	0.398(3)
6	0.81(1)	0.376(5)
8	0.77(1)	0.39(2)
10	0.76(1)	0.39(2)
16	0.72(1)	0.49(7)

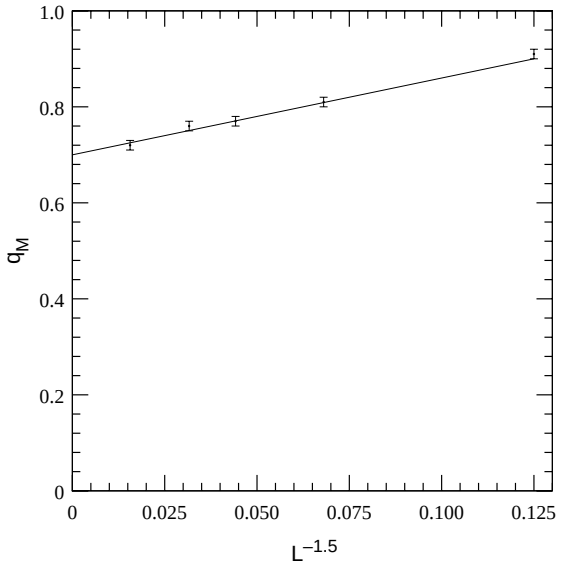

Figure 6. Value of the overlap q_{M} such that $P(q)$ is maximum (3D Ising spin glass). The continuous line is the fit described in the text. $T = 0.7$.

been extracted from an off-equilibrium simulation ($q \simeq 0.7$) [5]. The best (two-parameter) fit obtained by fixing $q_{\mathrm{M}} = 0.7$ (considered as an input from the dynamical simulations) gives compatible results with smaller errors. In figure 6 we show the q_{M} data versus $L^{-1.5}$ (see also table 2), and the curve from the best (two-parameter) fit.

From the numerical data for the 3D spin glass (these are taken from a state-of-the-art large-scale numerical simulation) we cannot exclude the possibility of $q_{\mathrm{EA}} = 0$ in the infinite-volume limit. We find that the best fit (that uses, in this case, only $L \geqslant 6$ data)

$$q_{\mathrm{M}} = (1.0 \pm 0.1)L^{-(0.12\pm0.02)} \tag{19}$$

is very good. So, even if the scenario of a non-zero overlap is favoured (the static value is equal to the dynamic one, the exponent of a decay to $q = 0$ is very small) in the 3D case we cannot use this limit to be sure of the existence of a phase transition with a non-zero order parameter (in 4D recent high statistical data established this evidence [8]). The safe evidence for the existence of a phase transition in the 3D spin glass relies, at the moment on the statistically significant crossing of the finite L Binder cumulant [3, 5], which revealed the fine details of the equilibrium probability distribution.

The behaviour of $P(0)$ also turns out to be the potential source of many ambiguities. We have seen that in the XY model it grows very slowly with the lattice size, in order to

asymptotically contribute to the $m_1 = 0$ delta function. In the 3D spin glass, where in a mean-field-like broken phase we expect a finite limit for $P(0)$, we also observe a constant plateau with a (not necessarily statistically significant) growth for $L = 16$. This behaviour contributes to falsify the droplet model picture, where one would expect $P(0)$ to decrease with the lattice size.

4. Conclusions

We have shown that the 2D ferromagnetic XY model and the 3D Ising spin glass finite-volume order-parameter probability distributions behave very similarly. The Binder cumulants on small lattice volumes show a similar *merging* at low T. Only on large lattices does the 3D spin glass exhibit a crossing typical of a phase transition. The results that we have discussed for the XY model are completely compatible with the KT predictions. We have analysed the finite-volume behaviour of the peak of the finite-volume order-parameter probability distribution. In the case of the XY model the preferred limit is zero. In the spin glass case the preferred value is non-zero, and compatible with an off-equilibrium estimate, but from the present data one cannot rule out the possibility of the position of the peak going to zero in the infinite-volume limit.

We have also established that $P(0)$ in the KT scenario has a finite-volume non-zero value, that increases in the infinite-volume limit. In the finite volume one can then exhibit probability distributions with the same shape as that of a finite-dimensional spin glass that has a trivial thermodynamic limit (a delta function in the origin). Analysing finite-size effects is crucial before reaching conclusions about the critical behaviour. In the 3D spin glass good evidence for the existence of a mean-field-like phase transition is based on a dynamical determination of the Edward–Anderson order parameter and on the crossing of the Binder cumulant on large lattices, but determining with good precision the shape of $P(q)$ on large lattice sizes will be important for making more details of the critical behaviour crystal clear.

Acknowledgments

DI acknowledges an FPU grant from MEC. JJR-L is supported by an EC HMC (ERBFMBICT950429) grant. We thank Paola Ranieri for many useful conversations.

References

[1] Rieger H 1995 *Annual Reviews of Computational Physics* vol II (Singapore: World Scientific) p 295
[2] Marinari E, Parisi G and Ruiz-Lorenzo J J 1997 Numerical simulations of spin glass systems *Spin Glasses and Random Fields* ed P Young (Singapore: World Scientific) in press, cond-mat/9701016
[3] Kawashima N and Young P 1996 *Phys. Rev.* B **53** R484
[4] Marinari E, Parisi G, Ruiz-Lorenzo J J and Ritort F 1996 *Phys. Rev. Lett.* **76** 843
[5] Marinari E, Parisi G and Ruiz-Lorenzo J J 1997 in preparation
[6] Mezard M, Parisi G and Virasoro M A 1987 *Spin Glass Theory and Beyond* (Singapore: World Scientific)
[7] Parisi G, Ricci Tersenghi F and Ruiz-Lorenzo J J 1996 *J. Phys. A: Math. Gen.* **29** 7943
[8] Marinari E and Zuliani F 1997 in preparation
[9] Binder K 1981 *Z. Phys.* B **43** 119
[10] Parisi G 1988 *Statistical Field Theory* (Redwood City, CA: Addison-Wesley)
[11] de Dominicis C, Kondor I and Temesvari T 1997 Beyond the Sherrington–Kirkpatrick model *Spin Glasses and Random Fields* ed P Young (Singapore: World Scientific) in press, cond-mat/9705215
[12] Green J E 1985 *J. Phys. A: Math. Gen.* **17** L43
[13] Franz S, Parisi G and Virasoro M A 1994 *J. Physique* I **4** 1657

[14] Wang J and Young A P 1993 *J. Phys. A: Math. Gen.* **26** 1063
[15] Parisi G, Ranieri P, Ricci-Tersenghi F and Ruiz-Lorenzo J J 1997 *J. Phys. A: Math. Gen.* **30** 7115
[16] Cugliandolo L, Kurchan J and Parisi G 1994 *J. Physique* I **4** 1691
[17] Gupta R and Bailie C F 1992 *Phys. Rev.* B **45** 2883
[18] Wolff U 1989 *Phys. Lett.* B **228** 3
[19] Battista C *et al* 1993 *Int. J. High Speed Comput.* **5** 637
[20] Marinari E and Parisi G 1992 *Europhys. Lett.* **19** 451
[21] Marinari E 1996 Optimized Monte Carlo methods *Lectures Given at the 1996 Budapest Summer School on Monte Carlo Methods* cond-mat/9612010
[22] Guerra F 1996 *Int. J. Mod. Phys.* B **10** 1675
[23] Iñiguez D, Parisi G and Ruiz-Lorenzo J J 1996 *J. Phys. A: Math. Gen.* **29** 4337
[24] Itzykson C and Drouffe J-M 1989 *Statistical Field Theory* (Cambridge: Cambridge University Press)